

# Effect of substance properties on the appearance and characteristics of repeated surface tension auto-oscillation driven by Marangoni force

N. M. Kovalchuk<sup>1</sup> and D. Vollhardt<sup>2,\*</sup><sup>1</sup>*Institute for Problems of Material Science, 03142 Kiev, Ukraine*<sup>2</sup>*Max Planck Institute of Colloids and Interfaces, 14424 Potsdam/Golm, Germany*

(Received 28 April 2003; published 28 January 2004)

The effect of substance properties (solution viscosity and density, surfactant bulk and surface diffusion coefficient, activity, and solubility) on the appearance and characteristics of surface tension auto-oscillation that occurs by dissolution of a surfactant drop under the water-air interface is considered in the framework of a simple mathematical model, taking into account the convection driven by the Marangoni effect and convective diffusion together with adsorption/desorption processes at the air-water interface. Numerical simulations show that apart from the Marangoni and Schmidt number, the system behavior is governed also by the exchange number, which determines the surfactant exchange with the interface. The criterion for the instability onset in a system with both normal and tangential (with respect to the interface) concentration gradient, the correlation between the global and local Marangoni numbers, as well as a comparison with experiment are discussed.

DOI: 10.1103/PhysRevE.69.016307

PACS number(s): 47.20.Dr, 47.20.Ma, 68.03.Cd, 05.65.+b

## INTRODUCTION

The dissipative patterns arising by energy and mass transfer in systems far from equilibrium have been the subject of scientific interest for many years. A canonical example of these is the Benard cells, which appear in thin liquid layers by heating from below [1]. Other examples of dissipative structures can be found elsewhere [2]. Primarily theoretical studies of the phenomena were performed on the basis of linear stability analysis [3–5]. It allows one to follow the system behavior near the bifurcation point and to find the critical value of the control parameter (the Rayleigh number for buoyancy-driven convective instability or the Marangoni number for convective instability driven by the gradient of the surface tension). For a more comprehensive study of the dissipative patterns, especially far from threshold, nonlinear effects should be taken into account [6–8].

There are, however, phenomena which can be understood only in the framework of the nonlinear dynamics because just nonlinear effects are crucial for their development [9]. An example is the nonlinear oscillations of the interfacial electrical potential and interfacial tension arising by the mass transfer through a liquid-liquid interface [10–16]. These oscillations can be a result of coupling of oscillating chemical reactions at the surface with hydrodynamic instability arising due to the Marangoni effect. But the contribution of each of these factors and the interaction between them has been unclear until now. Thus, there is no generally accepted mechanism of oscillations, despite a large variety of experimental investigations in this field, and one cannot predict in which other systems the resembling phenomenon may take place.

Auto-oscillation of the surface tension is a new, recently discovered phenomenon related to nonlinear surface dynamics [17]. It can be observed by the dissolution of a surfactant droplet having limited solubility in water placed on the tip of

a capillary under the free water interface. The necessary precondition for the development of repeated oscillations is the limited extensions of the free interface. The systems in which auto-oscillations take place are very simple from a chemical point of view because of the absence of chemical reactions. A middle chain aliphatic alcohol or a fatty acid can be used as a surfactant dissolving in water [18,19]. An example of oscillation is given in Fig. 1. Similar oscillations were generated at the water-nitrobenzene interface by the transfer of sodium dodecylsulphate (SDS) injected with a micro syringe in a point of the water bulk far from the interface [20].

On the basis of numerical simulations of the model system evolution, the mechanism for the development of repeated surface tension auto-oscillations was proposed in Ref. [21] and developed in Ref. [22]. The mathematical model describes the dissolution of a surfactant droplet situated at the tip of a capillary in a cylindrical vessel filled with water. It takes into account the convection driven by the Marangoni effect and convective diffusion together with adsorption/desorption processes at the air-water interface. The geometry of the model system and the main features of the fluid flow

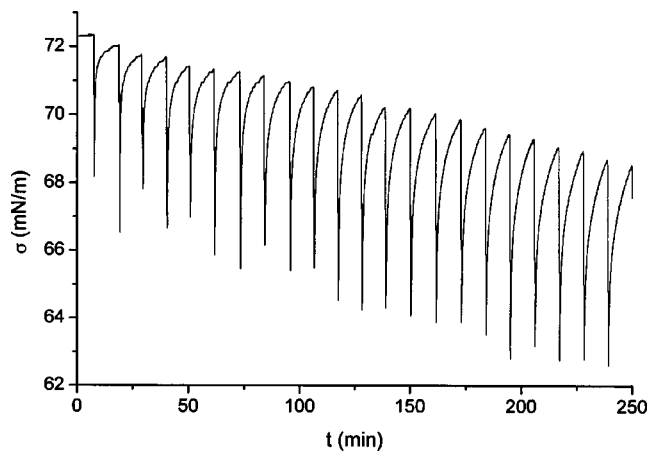


FIG. 1. Auto-oscillations of the surface tension in the system water-octanol (experimental results [19]).

\*Corresponding author.

during the oscillation are demonstrated in Fig. 4. During the induction period (before first oscillation), mainly diffusion mass transfer takes place in the system [21,22]. The surface motion due to nonuniform surfactant distribution forms the convective roll rotating in the direction from the capillary to the wall on the surface [direct convective roll, see Fig. 4(d)]. During the induction period, convection is too weak and its contribution to the mass transfer is negligible. At the same time, the increase of convective motion velocity leads to an increase of the surfactant supply to the surface, and therefore to an increase of the normal and tangential concentration gradients. The last causes a further increase of the surface velocity. So there is a feedback in the considered system that can support the convective instability development. When normal to the surface concentration gradient reaches the threshold value, the regime with predominance of diffusion mass transfer becomes unstable. Due to instability development, the system proceeds to the regime with predominance of the convective mass transfer. In the absence of buoyancy-driven convection, the instability arises in the considered system near the capillary where the normal concentration gradient has a maximum (this region will be referred to below as the instability region). Weak convective motion amplifies rapidly and convection extends in the bulk and propagates in the radial direction. Surfactant is supplied from the bulk to the interface in the region near the capillary and then convection spreads it over the whole interface. A sharp decrease of the surface tension is observed at this time.

When the concentration wave reaches the wall, the surfactant accumulates here and the reverse surface concentration gradient appears. It causes a decrease of the velocity of convective motion in this region. At the same time, near the capillary the surfactant is supplied to the interface and supports the direct concentration gradient here. Thus, the Marangoni force is directed to the wall near the capillary and is oppositely directed near the wall. Correlation of the concentration gradients near the capillary and near the wall determines the further evolution of the system. If the gradient near the capillary is stronger, the opposite gradient disappears with time, and a quasistationary convective regime with velocity slowly changing over time is established in the system [Fig. 4(d)]. In this case, the surface tension decreases monotonously after a single oscillation. Repeated oscillations do not develop in the system.

On the contrary, when the surface concentration gradient near the wall is large enough and is maintained during a sufficiently long time, it causes the surface motion in the direction from the wall to the capillary, i.e., the formation of the second convective roll, which rotates in the opposite direction relative to the former one, in the system [as shown in Fig. 4(a)]. Below, the second roll will be called the opposite or reverse convective roll. This opposite roll can extend to the capillary region [as in Fig. 4(b)] and break the surfactant supply from the droplet to the interface near the capillary. The convection fades at this time and the diffusion mass transfer becomes significant again [21]. The system returns to the slow stage of its evolution, which is a precondition for the development of repeated oscillation.

The correlation of the direct and the opposite surface con-

centration gradients and, as a consequence, the appearance of regimes with single or repeated oscillations, as well as the characteristics of auto-oscillations, depend on the system geometry (mainly on the vessel radius and immersion depth of the capillary) and on the properties of the solute and solution. The effect of the geometrical characteristics (radius and depth of the vessel, immersion depth of the capillary, droplet size) was reported in Ref. [22]. The effect of the substance properties is discussed below.

## MATHEMATICAL FORMULATION

The mathematical model and the numerical scheme used in this study are the same as given in Ref. [21]. The model system represents a cylindrical container filled with a viscous incompressible Newtonian liquid. The upper liquid surface is in contact with a passive gas. A cylindrical capillary with a spherical surfactant droplet on the tip is situated in the liquid so that the capillary axis coincides with the container axis. The density of the solution is supposed independent of the concentration, and, therefore, the buoyancy effect is not taken into account. The independence of the variables of the angular coordinate is assumed according to the experimental observations. The system evolution is described by Navier-Stokes, continuity, and convective diffusion equations rewritten in terms of vorticity and stream function in cylindrical coordinates. By scaling the time, length, velocity, concentration, stream function, and vorticity correspondingly with  $L^2/D$ ,  $L$ ,  $D/L$ ,  $c_0$ ,  $LD$ , and  $D/L^2$ , the dimensionless form of the governing equations is

$$\frac{\partial \omega}{\partial t} + \frac{\partial(v_r \omega)}{\partial r} + \frac{\partial(v_z \omega)}{\partial z} - \text{Sc} \left( \frac{\partial^2 \omega}{\partial r^2} + \frac{\partial^2 \omega}{\partial z^2} + \frac{1}{r} \frac{\partial \omega}{\partial r} - \frac{\omega}{r^2} \right) = 0, \quad (1)$$

$$\frac{\partial^2 \Psi}{\partial r^2} + \frac{\partial^2 \Psi}{\partial z^2} - \frac{1}{r} \frac{\partial \Psi}{\partial r} - \omega r = 0, \quad (2)$$

$$\frac{\partial c}{\partial t} + \frac{\partial(v_r c)}{\partial r} + \frac{\partial(v_z c)}{\partial z} + \frac{v_r c}{r} - \left( \frac{\partial^2 c}{\partial r^2} + \frac{\partial^2 c}{\partial z^2} + \frac{1}{r} \frac{\partial c}{\partial r} \right) = 0, \quad (3)$$

where  $L$  is the characteristic length scale,  $D$  is the bulk diffusion coefficient of the surfactant,  $c_0$  is the surfactant solubility,  $t$  is the time,  $r$  is the radial coordinate,  $z$  is the normal to the interface coordinate down directed with  $z=0$  on the interface,  $v_r$  and  $v_z$  are the velocity components in radial and normal to the interface directions, respectively,  $\Psi$  is the stream function, defined so that  $v_r = (1/r)(\partial \Psi / \partial z)$  and  $v_z = - (1/r)(\partial \Psi / \partial r)$ ,  $\omega = (\partial v_r / \partial z) - (\partial v_z / \partial r)$  is the vorticity,  $\text{Sc} = \mu / \rho D$  is the Schmidt number (diffusion Prandtl number),  $\mu$  is the dynamic viscosity of the liquid,  $\rho$  is the liquid density, and  $c$  is the surfactant concentration.

In the initial state, the liquid is supposed motionless. The dimensionless surfactant concentration is equal to unity at the droplet/water interface and is equal to zero elsewhere. No-slip boundary conditions are used for the container wall and bottom, for the capillary, and the droplet surface. The

gas-liquid interface is supposed nondeformable. The intrinsic surface viscosity as well as the evaporation of the solution are neglected. The diffusion-controlled adsorption kinetics is assumed. The surfactant mass balance on the free surface is described by the equation

$$\frac{\partial \Gamma}{\partial t} + \frac{\partial(\Gamma v_r)}{\partial r} + \frac{\Gamma v_r}{r} - \frac{D_s}{D} \left( \frac{\partial^2 \Gamma}{\partial r^2} + \frac{1}{r} \frac{\partial \Gamma}{\partial r} \right) - N_E \frac{\partial c}{\partial z} = 0$$

at  $z=0$ . (4)

Here  $K_L$  and  $\Gamma_m$  are the parameters of the Langmuir isotherm,  $D_s$  is the surface diffusion coefficient, and  $\Gamma$  is the Gibbs adsorption scaled by  $c_0 K_L \Gamma_m$ .  $N_E = L/K_L \Gamma_m$  is the dimensionless parameter, referred to below as the exchange number. It determines the effect of surfactant exchange between the surface and bulk.  $N_E \rightarrow 0$  corresponds to the limiting case of an insoluble monolayer when the exchange with the interface is absent.

The boundary condition for the vortex on the free surface is obtained from the tangential stress balance by using the Szyszkowsky-Langmuir equation for the surface tension dependence versus surface concentration (adsorption),

$$\omega = \text{Ma} \frac{1}{(1 - K_L c_0 \Gamma)} \frac{\partial \Gamma}{\partial r} \quad \text{at } z=0. \quad (5)$$

Here  $\text{Ma} = RTc_0 K_L \Gamma_m L / \mu D$  is the Marangoni number,  $R$  is the gas constant, and  $T$  is the temperature.

Four dimensionless characteristic numbers, namely the Schmidt number, the Marangoni number, the ratio of the surface to bulk diffusion coefficients, and the exchange number (the ratio of the characteristic length scale for the considered system to the characteristic adsorption length  $K_L \Gamma_m$ ), determine the system behavior. These characteristic parameters depend on the surfactant and the solution properties as well as on the temperature and the system length scale. The computation domain is determined by the ratios of the system dimensions to the characteristic length. Thus, the dependence on the system geometric characteristics is also assumed. The effect of the geometric characteristics on the development of the auto-oscillations of the surface tension is investigated in Ref. [22]. In the presented study, a system with invariable geometry is considered: cell radius  $R = 20$  mm, cell height  $H = 20$  mm, capillary immersion depth  $h = 8$  mm, capillary radius  $r_c = 1$  mm, droplet radius  $r_0 = 1.5$  mm, and characteristic length  $L = 20$  mm. The values of the surface tension and surface velocity, given in the next section, are calculated for the distance  $r = 10$  mm from the capillary axis. It is accepted that  $D_s/D = 1$  unless the other is not stated.

Initially the effect of the dimensionless characteristic numbers on the system behavior will be considered, and then the influence of the solute and solution properties will be discussed as well. It is noteworthy that the used dimensionless numbers are independent of each other. Therefore, it is possible to vary each of them keeping the other constant. Separately the role of the multiplier  $1/(1 - K_L c_0 \Gamma) = (1 + K_L c_0 c)|_{z=0}$ , which appears in Eq. (5) and depends on the parameter  $K_L c_0$ , will be considered. In contrast to the char-

acteristic numbers defined above, this multiplier depends on the radial coordinate and changes with time in accordance with changes of the dimensionless concentration values. The effect of this multiplier will be discussed together with the influence of substance properties.

For convenience, the results of calculations by discussion of the characteristic number effect are presented in dimensional form for the values of time, velocity, and surface tension, accepting the following values of the surfactant characteristics (corresponding to the properties of the system octanol-water): solubility of the surfactant  $c_0 = 3.4$  mol/m<sup>3</sup>, parameters of the Langmuir isotherm  $K_L = 3.23$  m<sup>3</sup>/mol,  $\Gamma_m = 6.6 \times 10^{-6}$  mol/m<sup>2</sup>, and volume diffusion coefficient  $D = 6.7 \times 10^{-10}$  m<sup>2</sup>/s. The values of the dimensionless parameters for the octanol-water system (solution density  $\rho = 1$  g/cm<sup>3</sup>, solution viscosity  $\mu = 0.01$  g/cm/s, temperature  $T = 298$  K) are  $\text{Sc} = 1500$ ,  $\text{Ma} = 5.4 \times 10^9$ , and  $N_E = 940$ .

The numerical simulation was performed on the basis of the finite-difference method. Equation (2) was solved by the Gauss-Seidel iterative method. The two-point forward-difference approximation is used for equations of vortex and solute transfer. Convergence of the numerical scheme and the proper grid resolution was implemented by comparison of the simulation results for different grids [21].

## RESULTS AND DISCUSSION

### Schmidt number

The Schmidt number (diffusion Prandtl number) determines the correlation of viscous and inertial terms in the Navier-Stokes Eq. (1). The lower the Schmidt number is, the less is the change of the bulk vorticity values caused by a given driving surface force. That means that a decrease of Schmidt number leads to a weakening of the feedback between the concentration gradients and the intensity of convective motion in the considered system, and, therefore, to a decrease of the achieved velocities and of the amounts the surfactant supplied to the surface. On the other hand, that means that the formation and expansion of the reverse convective roll will be more difficult at small values of the Schmidt number because of the large inertia of motion in the direct convective roll. Thus, one can expect that at Schmidt numbers less than a certain critical value, the repeated oscillations do not appear in the considered system. These assumptions are confirmed by the performed numerical simulations. Some calculated characteristics of oscillations for different Schmidt numbers are presented in Table I.

As discussed in the Introduction, the diffusion mass transfer dominates during the induction period. The change of Schmidt number influences only the development of convective motion in the system. That is why the induction period is practically independent of the Schmidt number. The induction period decreases only very insignificantly with an increase of the Schmidt number in accordance with an increase of the velocity.

The maximum of the surface velocity and the oscillation amplitude increases with an increase of the Schmidt number, as was expected. It was established by a study of the system geometry effects on the auto-oscillations development that at

TABLE I. Dependence of the auto-oscillation characteristics on the Schmidt number ( $Ma=5.4\times 10^9$ ,  $N_E=940$ ).

Sc	Induction period (min)	Oscillations period (min) <sup>a</sup>	Oscillations amplitude (mN/m) <sup>b</sup>	Maximum positive velocity value (mm/s) <sup>b</sup>	Maximum negative velocity value (mm/s) <sup>b</sup>
150	31.7		2.7/	4.1/	
300	31.5	42	3.2/2.8	4.7/0.57	0.006/0.0135
600	31.4	38	3.7/3.1	5.7/0.67	0.017/0.0165
1500	31.3	36	4.3/3.5	7.4/0.79	0.013/0.0177
15 000	31.2	38	5.2/4.1	12.9/0.97	0.011/0.0174

<sup>a</sup>The mean value for the third to sixth oscillations.

<sup>b</sup>Numerator, for the first oscillation; denominator, the mean value for the third to sixth oscillations.

large enough values of the surface velocity in the direct roll, the reverse surface concentration gradient, induced near the wall, becomes insufficient to overcome the inertia of the convective motion directed from the capillary to the wall. Thus, the maximal value of the negative surface velocity, reached in the reverse roll after the first oscillation, decreases with an increase of positive velocity in the direct roll, and, at a certain value of positive velocity, the reverse convective roll does not reach the capillary. The system passes from the regime with repeated oscillations to those with only a single oscillation. The reverse convective roll does not appear at all by a further increase of the maximum surface velocity.

The results of numerical simulations show that an increase of positive velocity due to an increase of the Schmidt number, similarly to the case of the geometry change, causes a decrease of negative velocities achieved in the reverse convective roll for large enough velocities ( $Sc=600-15\,000$  for the first oscillation,  $Sc=1500-15\,000$  for the following oscillations). But according to reinforcement of the feedback in the system, this decrease is rather slow, and one could expect that there is no maximum critical Schmidt number. At the same time, the effect of a feedback weakening is more important than the effect of a positive velocity decrease, and, therefore, there is a minimal critical value of Schmidt number below which only a single oscillation appears in the system.

During the fast stage of the system evolution, a large amount of the surfactant is spread over the surface. As a result, the concentration at most of the surface becomes larger than the concentration in the underlying bulk solution. The exception is only a small area near the capillary where the surfactant is supplied to the surface. The amount of the supplied surfactant is determined by the velocity of the bulk convection. The decrease of the velocities leads to a decrease of the surfactant supply to the surface due to convection. The decrease with time of the bulk velocity is defined by the Schmidt number. The analysis of the numerical results displays that the bulk velocity decreases practically with the same rate as the surface velocity for  $Sc=15\,000$ , however it decreases much slower for smaller Schmidt numbers. For example, in the time interval when the surface velocity at the point with coordinate  $r=0.225$  cm decreases ten times, the bulk velocity in the point  $r=0.225$  cm,  $z=0.225$  cm decreases only three times for  $Sc=150$ . That is why the surface

concentration gradients in the capillary region decrease much more slowly with time at small Schmidt numbers. That leads to a delay of the surface velocity decrease in the direct roll (Fig. 2). As a result, the positive tangential concentration gradient and the maximum positive surface velocity at the moment, when the reverse roll appears, are larger when the Schmidt number is smaller (for example, the positive surface velocity by appearance of the reverse convective roll for  $Sc=150$  is two times larger than for  $Sc=15\,000$ ). Therefore, at a small enough value of Schmidt number, the reverse convective roll cannot overcome the convective motion directed from the capillary to the wall, and repeated oscillations do not appear in the system.

It should be noted that the critical value of one of the dimensionless parameters depends on the others. For example, when the aspect ratio of the system (ratio of the cell radius to the capillary immersion depth) decreases from 2.5 to 2, the repeated oscillations appear also for  $Sc=150$ . Thus, the decrease of the aspect ratio of the system leads to a decrease of the critical value of the Schmidt number, and, correspondingly, the decrease of the Schmidt number leads to a decrease of the critical aspect ratio. The decrease of the

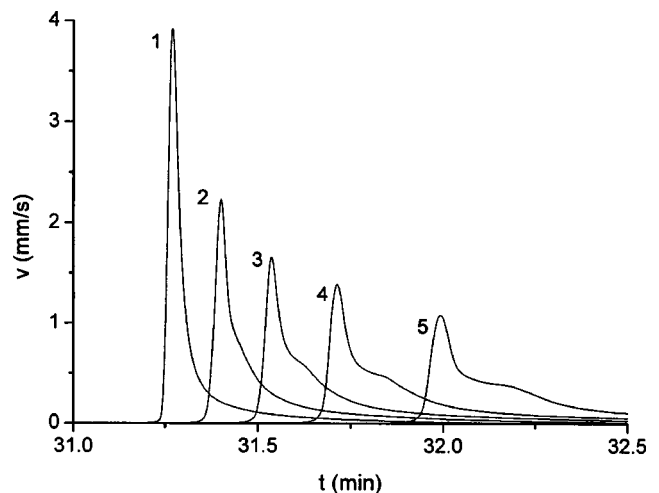


FIG. 2. The surface velocity vs time during the first oscillation for different Schmidt numbers: 1,  $Sc=15\,000$ ; 2,  $Sc=1500$ ; 3,  $Sc=600$ ; 4,  $Sc=300$ ; 5,  $Sc=150$ . The distance from the vessel axis  $r=1.875$  cm.

TABLE II. Dependence of the auto-oscillation characteristics on the Marangoni number ( $Sc=1500$ ,  $N_E=940$ ).

Ma	Induction period (min)	Oscillations period (min) <sup>a</sup>	Oscillations amplitude (mN/m) <sup>b</sup>	Maximum positive velocity value (mm/s) <sup>b</sup>	Maximum negative velocity value (mm/s) <sup>b</sup>
$5.4 \times 10^7$	48.4	44	6.8/4.1	1.5/0.74	0.017/0.0196
$5.4 \times 10^8$	38.3	38	5.5/3.6	3.5/0.79	0.014/0.0184
$5.4 \times 10^9$	31.3	36	4.3/3.5	7.4/0.79	0.013/0.0177
$5.4 \times 10^{10}$	26.2	35	3.5/3.4	13.8/0.79	0.011/0.0163

<sup>a</sup>The mean value for the third to sixth oscillations.

<sup>b</sup>Numerator, for the first oscillation; denominator, the mean value for the third to sixth oscillations.

Marangoni number also leads to a decrease of the critical value of the Schmidt number.

### Marangoni number

The Marangoni number appears in the nondimensional form of the surface tangential stress balance equation (5). It determines the velocity change due to the tangential concentration gradient at the surface. The Marangoni number introduced above is written in the form that does not include the concentration gradient. Actually the ratio of the surfactant solubility to the characteristic length scale  $c_0/L$  replaces it. Thus the Marangoni number in the form  $Ma = RTc_0K_L\Gamma_mL/\mu D$  describes the system as a whole and does not account for the fact that concentration gradients in the considered system are functions of the coordinates and time [ $c=c(r,z,t)$  and  $\nabla c=\nabla c(r,z,t)$ ]. It controls the “macroscopic” system behavior, i.e., it determines the possibility of repeated oscillations of surface tension and their characteristics. Dependence of the oscillation characteristics on the global Marangoni number is given in Table II. Repeated oscillations exist in all ranges of the studied parameter values (simulation of the system behavior by the larger values of the Marangoni number was not performed because of the convergence problems of the accepted numerical scheme). The global Marangoni number affects both the oscillation period and the amplitude. Its influence is especially strong for characteristics of the first oscillation. To understand these dependences, let us consider the system evolution in more detail.

As a rule, the appearance of instability by heat or mass transfer through the liquid/liquid interface is considered in the presence of temperature or concentration gradients only normal to the interface. It is well known [1–3] that in this case, the diffusion regime can become unstable (because of feedback between the temperature or concentration gradients and velocity growth), and the system passes to the regime with more intensive convective mass transfer. Such a transition takes place when a concentration gradient exceeds a certain threshold value. The threshold value depends on the system geometry and the substance properties. When the Marangoni effect (appearance of the convective motion due to a gradient of the surface tension) is the driving force for the instability by solute transfer, the value of the Marangoni

number  $Ma = (L/\mu D)(\partial\sigma/\partial c)\text{grad}c$  determines the onset of instability.

The system presented here differs from that described above by the presence of both the component normal to the surface and the tangential component of the concentration gradient. Besides, the concentration distribution and, therefore, the concentration gradients in the system change with time and are nonuniform in space. Convection develops in this system already in the induction period due to the tangential surface concentration gradient, but this convection is very slow and its contribution to the mass transfer is negligible [21]. Thus, during the induction period, the state of the system can be characterized as a quasistationary convective regime with a predominance of diffusion mass transfer. An abrupt decrease of the surface tension in the system is accompanied by fast convective motion with a predominance of convective mass transfer. The system transition from the regime with a predominance of diffusion mass transfer to the regime with a predominance of convective mass transfer occurs due to the rise of instability. It is clear from the very sharp increase of the surface velocity after a long period of its relatively slow increase, as illustrated by Fig. 3(a). The dashed line shows the increase of velocity in the absence of instability. The instability can only arise in the considered system similarly to the classical examples if the normal concentration gradient near the surface is large enough to support the fast growth of the tangential concentration gradient at the surface and, consequently, the fast growth of the surface velocity. The Marangoni number can be taken as a criterion of instability. However, in the considered system the normal concentration gradient near the surface depends on the radial coordinate. Thus the introduction of a local Marangoni number is needed. Presenting the derivative  $d\sigma/dc$  in explicit form, it can be written

$$\begin{aligned}
 Ma_{\text{local}} &= \frac{RTK_L\Gamma_mL^2}{\mu D} \left. \frac{\partial\tilde{c}}{\partial\tilde{z}} \right|_{\tilde{z}=0} \\
 &= \frac{RTc_0K_L\Gamma_mL}{\mu D} \frac{\partial c}{\partial z} \\
 &= Ma \left. \frac{\partial c}{\partial z} \right|_{z=0}, \tag{6}
 \end{aligned}$$

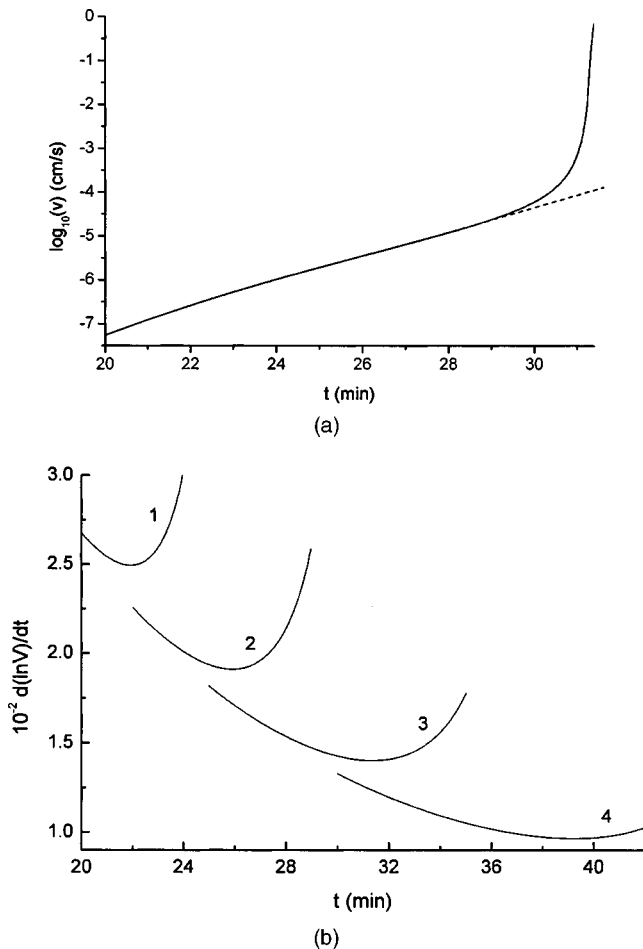


FIG. 3. Convection in the system during the induction period and the onset of instability: *a*, time dependence of surface velocity for  $Ma=5.4 \times 10^9$ ; *b*, time dependence of the velocity growth rate: 1,  $Ma=5.4 \times 10^{10}$ ; 2,  $Ma=5.4 \times 10^9$ ; 3,  $Ma=5.4 \times 10^8$ ; 4,  $Ma=5.4 \times 10^7$ .

where  $\partial \bar{c} / \partial \bar{z}$  is the dimensional and  $\partial c / \partial z$  the dimensionless concentration gradient. It is seen that the so-defined parameter  $Ma_{local}$  is not a number for the considered system, as it varies with the radial coordinate and time.  $Ma_{local}$  has a maximum in the capillary region. That is why the instability begins to develop here. The critical value of this parameter depends on the concentration gradients in other points of the surface as well as on the velocity distribution over the surface. During the induction period, the convective fluxes in the system are rather small in comparison to diffusional and, therefore, the influence of the convection on the surfactant distribution is also small. Thus, it can be supposed that the critical value of the parameter  $Ma_{local}$  depends only weakly on the global Marangoni number at least at the onset of the first oscillation.

To prove this assumption, first a convenient criterion for the time moment of the instability onset in the considered system should be chosen. The difficulty in establishing such a criterion is caused by the presence in the system of increasing convective motion due to the tangential concentration gradient. The instability development leads to a rapid increase of  $Ma_{local}$  and to very large values of the velocity

TABLE III. Dependence of the time of instability onset and critical values of the local Marangoni number on the global Marangoni number of the system.

Ma	$t_{inst}$ (min)	$Ma_{local}$ (critical)
$5.4 \times 10^7$	39.0	440
$5.4 \times 10^8$	31.4	580
$5.4 \times 10^9$	25.9	700
$5.4 \times 10^{10}$	21.9	820

growth rate because of the existence of a feedback in the system. At the same time, near the threshold the growth rate of the velocity due to instability is still close to zero and cannot be separated from the growth rate of the stable convective motion. The time moment of the instability onset, however, can be estimated due to the fact that the growth rate of the stable convection in the considered system decreases with time. The time dependences of the velocity growth rate for the  $Ma$  values given in Table III are presented in Fig. 3(b). Obviously time moments of the curves minima can be accepted as estimated (from above) values for the instability onset. The corresponding values are given in Table III.

It is seen from Table III that indeed the critical values of the local Marangoni number depend rather weakly on the global Marangoni number. Therefore, the larger the global Marangoni number is, the less is the normal concentration gradient desired for the instability onset and the less is the induction period. Note that the values of the induction period given in Tables I, II, and IV correspond (in accordance with the terminology of the experimental study) to the appreciable change of the surface tension, which is conveniently chosen here at the level  $10^{-3}$  mN/m. Comparison of  $t_{inst}$  and induction period (Tables III and II) shows that for larger  $Ma$  values the instability develops more rapidly and leads more quickly to the noticeable change in the surface tension. It is noteworthy that the maximum achieved by  $Ma_{local}$  during an oscillation is some order larger than its critical value. It causes large values of the growth rate, which lead to sharp velocity peaks [cf. Fig. 6(b) below].

The system behavior during the second and following oscillations is more complicated. The oscillation period can be divided into four stages (starting from the moment of the surface velocity maximum): (i) a decrease of the surface velocity and a rise of the reverse convective roll and its extension to the capillary; (ii) a building (mainly due to diffusion from the drop) of normal concentration gradient near the surface sufficient to stimulate growth of the velocity in the direct convective roll; (iii) growth of the velocity in the direct convective roll, accompanied by its extension to the wall and reducing the reverse convective roll; (iv) fast velocity growth after a disappearance of the reverse convective roll. Let us consider the relative duration of the various stages, taking as an example the fourth oscillation (the period of the fourth oscillation changes from 35 to 45 min depending on the Marangoni number). The first stage lasts nearly 5–6 min independently of the Marangoni number. Hydrodynamic behavior of the system during this stage is clear from Fig. 4. Figure 4(a) displays the appearance of the reverse convective

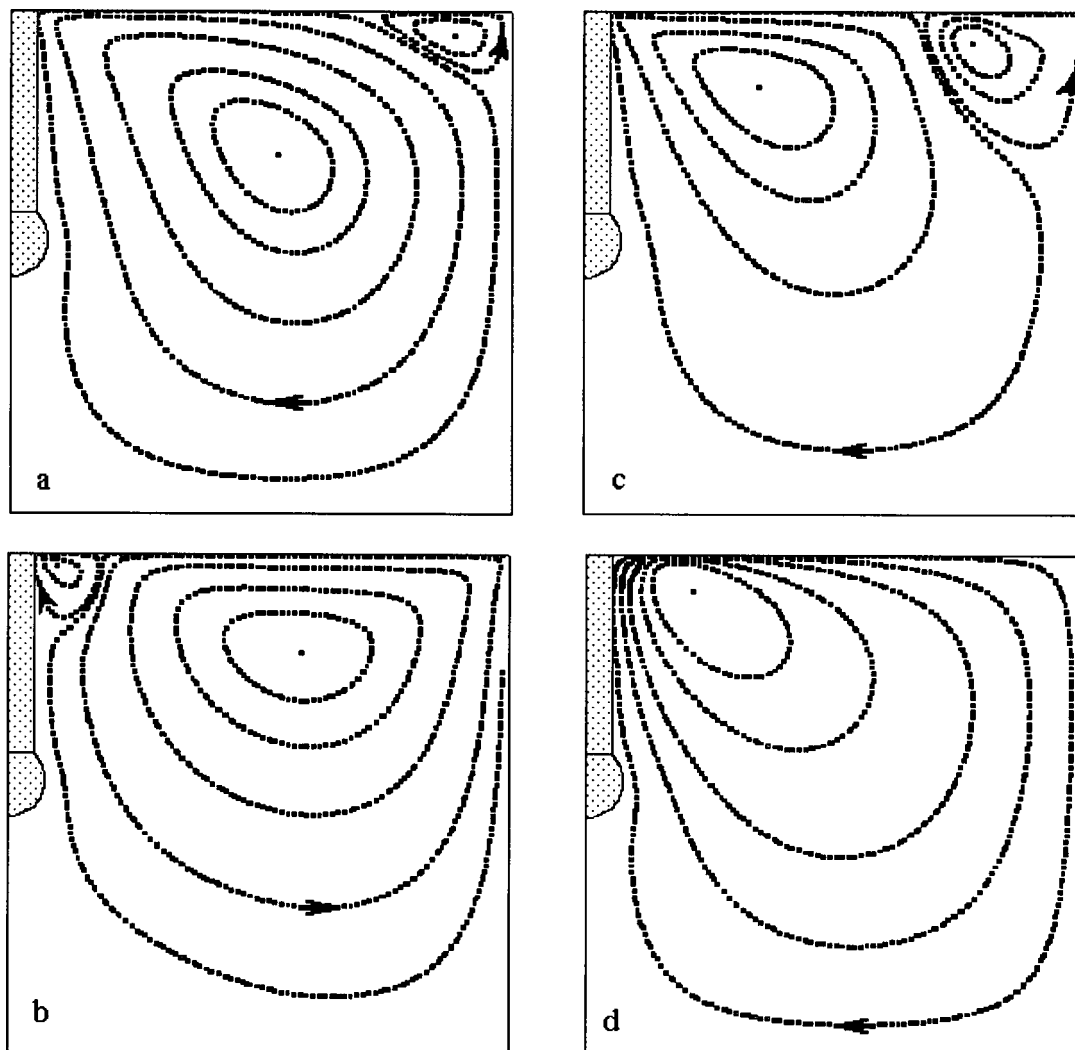


FIG. 4. Streamlines distribution in the bulk during the oscillation period (for details, see text). The computational domain represents the radial section of a cylindrical vessel with capillary and surfactant droplet.

roll near the wall, and Fig. 4(b) corresponds to the moment when it is already extended to the capillary. The larger  $Ma$  is, the smaller is the velocity maximum reached in the reverse roll (Table II). The time needed to build up the normal concentration gradient near the capillary sufficiently to cause the surface velocity growth, i.e., the second stage, is rather short as compared to the oscillations period (about 3 min), and is practically independent of the Marangoni number. The stream lines distribution during this stage corresponds to that given in Fig. 4(b). The convective motion in the system is the most weak at this time. The smaller the Marangoni number is, the smaller is the minimum of the positive surface velocity value near the capillary.

The third stage is the longest. During this stage, the velocity on the part of the surface, involved in the positive roll, increases very slowly because of the interaction with the reverse roll. The system passes from the dynamic state presented in Fig. 4(b), through the state presented in Fig. 4(c), to the state presented in Fig. 4(d), where only the direct convective roll remains. The duration of the third stage increases from about 25 min for  $Ma=5.4 \times 10^{10}$  to about 35 min for

$Ma=5.4 \times 10^7$  due to a decrease of the positive surface velocity minimum and the tangential stress with a decrease of the Marangoni number. Thus, the decrease of the oscillation period with an increase of  $Ma$  is due to a quicker extension of the positive and contraction of the negative convective roll.

After the disappearance of the reverse convective roll, the velocity in the direct roll increases rather quickly to the maximum value. This stage of the oscillation period is rather short (about 2 min) and is independent of the Marangoni number. As the total time of the velocity growth decreases with an increase of  $Ma$ , it appears that the maximum of the velocity value is practically independent of the Marangoni number (Table II).

Data given in Table II show that the oscillation amplitude increases with a decrease of the Marangoni number. But one should keep in mind that these data represent in fact dimensionless values scaled for convenience of presentation by a prior chosen value of  $c_0 K_L \Gamma_m$  (see the end of the section on mathematical formulation). In the case when the decrease of

TABLE IV. Dependence of the auto-oscillation characteristics on the exchange number ( $Sc=1500$ ,  $Ma=5.4 \times 10^9$ ).

$N_E$	Induction period (min)	Oscillations period (min) <sup>a</sup>	Oscillations amplitude (mN/m) <sup>b</sup>	Maximum of velocity value (mm/s) <sup>b</sup>	Minimum of velocity value (mm/s) <sup>b</sup>
47 <sup>c</sup>	35.5		2.6/	2.6/	0.0027/
94	34	41	3.3/0.8	3.3/0.027	0.0043/0.0072
190	32.9	21	3.9/0.4	4.2/0.045	0.0027/0.023
330	32.2	99	4.2/6.3	5.0/0.34	-0.0015/-0.008
470	31.8	75	4.3/5.5	5.9/0.47	-0.005/-0.0111
940	31.3	36	4.3/3.5	7.4/0.79	-0.013/-0.0177
9400	30.6	9	3.2/0.7	19.3/2.67	-0.083/-0.068
33 000	30.5	6	2.3/0.3	36.5/4.3	-0.129/-0.1
47 000	30.5		1.7/	45.0/	-0.144/
94 000	30.4		0.6/	62.8/	0.08/

<sup>a</sup>The mean value for the third to sixth oscillations.

<sup>b</sup>Numerator, for the first oscillation; denominator, the mean value for the third to sixth oscillations.

<sup>c</sup>Values for the repeated oscillation are not shown because of the big difference in the characteristics of small- and large-amplitude oscillations (see Fig. 6, curve 6).

the Marangoni number is due to a decrease, for example, of  $c_0$ , the dimensional oscillation amplitude decreases, and at a certain small  $Ma$  the oscillations can even become undetectable in experiments.

With decreasing Marangoni number  $Ma$ , the critical Schmidt number decreases and the critical aspect ratio increases.

**Effect of the exchange number**

The characteristics of the auto-oscillations in dependence on the exchange number are given in Table IV. The dimensionless parameter  $N_E=L/K_L\Gamma_m$  determines the intensity of the normal diffusion flux to or from the surface. The larger  $N_E$  is, the larger is the surfactant flux at a certain normal concentration gradient. At the same time, the parameter influences the value of the normal concentration gradient, especially during the induction period. The normal surface concentration gradient (related to the same time moments) decreases with an increase of the exchange number, which is illustrated in Fig. 5(a).

It was also found (accepting the same criterion for the instability onset as in the previous section) that the critical value of the normal concentration gradient and consequently the local Marangoni number for the first oscillation is approximately inversely proportional to the exchange number (by keeping  $Sc$  and  $Ma$  constant). In other words, the instability arises in the considered system when a surfactant flux to the interface,  $N_E\partial c/\partial z$ , exceeds a threshold value that is almost independent of the exchange number. That is why the instability arises at rather similar times in the systems with different  $N_E$ , i.e., this parameter has only a small influence on the induction period value. The induction period decreases only slightly with an increase of the exchange number in all ranges of the studied parameter values.

At the instability onset, a correlation of convective and diffusional surfactant transfer in the instability region is prac-

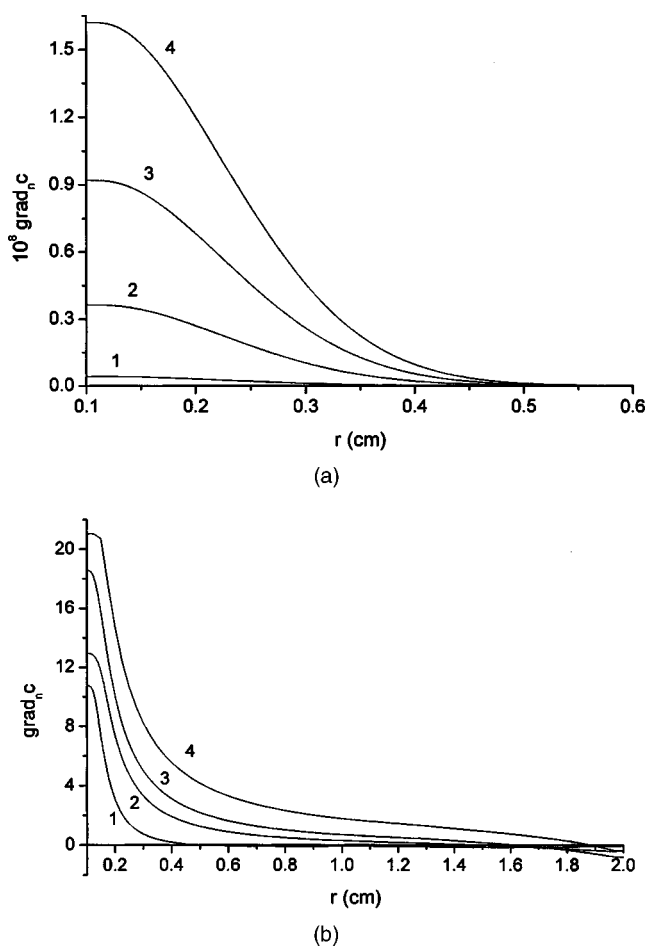


FIG. 5. Radial distribution of the dimensionless normal concentration gradient for  $Ma=5.4 \times 10^9$ ,  $Sc=1500$ : a, for  $t=20$  min; 1,  $N_E=9400$ ; 2,  $N_E=9400$ ; 3,  $N_E=280$ ; 4,  $N_E=94$ ; b, for the time moments, when the normal concentration gradient reaches its maximum; 1,  $N_E=94000$ ; 2,  $N_E=9400$ ; 3,  $N_E=940$ ; 4,  $N_E=94$ .

tically independent of the exchange number. The convective fluxes are on average 0.1% of the diffusional fluxes. The growth rate of the velocity is small at the instability onset and increases rather slowly. Only when convective fluxes become larger than diffusional does the instability develop very quickly. The normal concentration gradient becomes less dependent on  $N_E$  in this stage due to convective supply of the surfactant [Fig. 5(b)]. Thus the surfactant flux to the interface becomes larger the larger the value of  $N_E$  is. That is why the velocity increases more rapidly and reaches larger values for larger exchange numbers. All the other processes occur more quickly in systems with large  $N_E$ , particularly when fading of instability. The period of the repeated oscillations depends strongly on the exchange number because the convection plays a more important part at this time than during the induction period; moreover, the convective fluxes are larger for larger values of  $N_E$ .

The essential increase of the surface concentration also corresponds to the time when convective fluxes begin to exceed the diffusional. Oscillation amplitude is determined by the value of the surfactant flux, by the area where the flux is directed to the surface, and by the time during which the surfactant is supplied to the interface. The surfactant flux is larger the larger the exchange number is. The duration of the surfactant supply decreases with an increase of the exchange number. For example, the time between the beginning of the essential change of the surface tension (i.e., the end of induction period) and the moment of minimum value of the surface tension for  $N_E=940$  is about three times larger than for  $N_E=9400$ . The area through which the surfactant supply takes place decreases with an increase of the exchange number as well [Fig. 5(b)]. As a result of the common action of these factors, the nonmonotonous dependence of the oscillation amplitude on the exchange number takes place (Table IV).

The way in which the system goes to equilibrium depends essentially on the exchange number, which is illustrated in Fig. 6. At large parameter values, a regime with a single oscillation takes place (Fig. 6, curve 1). The surface velocity in this regime is too large and cannot be suppressed by the reverse concentration gradient. With decreasing  $N_E$ , several oscillations appear in the system before it passes to the nonoscillating (continuous) regime (Fig. 6, curve 2). The maximum surface velocity decreases and the oscillation amplitude increases with a decrease of exchange number. Already in the case given in Fig. 6, curve 2, the amount of the surfactant spread over the interface after the first oscillation is enough to build up the sufficient reverse concentration gradient, and the amount of the surfactant supplied to the wall region beneath the surface is sufficient to support the reverse gradient during the time needed to create a strong reverse convective roll. The repeated oscillation appears in the system. But these are transient oscillations with rather small amplitude, during which the mean value of the surface tension increases with time. By appearance of the oscillation with larger amplitude characterized also by a larger surface velocity (the fifth oscillation in Fig. 6, curve 2), the amount of the surfactant accumulated in the wall region becomes insufficient to hold the reverse concentration gradient during

a long time. The reverse convective roll does not propagate to the capillary region and the system passes to the nonoscillatory regime. By a further decrease of the exchange number, the system passes to the regime with stable repeated oscillations, and just after the oscillation with larger amplitude, the common oscillation with gradually decreasing mean value of the surface tension begins instead of the transient oscillation. The transient oscillations disappear completely at smaller  $N_E$  values (Fig. 6, curve 3). Regimes with repeated oscillations exist by parameter variation in a wide range. It is seen from Table IV that the maximum of the negative velocity decreases with the decrease of exchange number, and eventually the situation is reached when the reverse convective roll does not propagate to the capillary. The system passes to the regime with damping oscillations (Fig. 6, curve 4). The further decrease of the exchange number leads to a decrease of the damping due to a decrease of the surfactant flux to the interface, and after some oscillation of the small amplitude and nearly symmetrical shape, the oscillation of the larger amplitude typical for the auto-oscillation asymmetrical shape appears in the system (Fig. 6, curve 5). The reverse convective roll begins to extend again to the capillary region. The regime with large oscillation amplitude appears earlier by a further decrease of the exchange number (Fig. 6, curve 6). The average oscillation characteristics for the regime, corresponding to curve 6 in Fig. 6, are not given in Table IV because of a too big difference in the characteristics of small- and large-amplitude oscillations. The range of  $N_E$  values corresponding to the fading oscillations regime increases with a decrease of the Schmidt number and with an increase of the Marangoni number. Transition to the nonoscillating regime (at large exchange numbers) shifts to smaller  $N_E$  values when the Marangoni and Schmidt numbers decrease.

#### Effect of the parameter $D_s/D$

The parameter  $D_s/D$  determines the intensity of the surface diffusion. An increase of  $D_s/D$  promotes the smoothing of the surface concentration gradients and leads to system stabilization. At the same time, the calculations show that the contribution of the surface diffusion to the surface mass balance is rather small, i.e., the surface diffusion fluxes at  $D_s/D=1$  are some orders of magnitude less than the fluxes due to the surface convection and diffusion from the bulk. An increase of  $D_s/D$  up to 1000 leads only to a small increase of the induction period (about 7%) and oscillation period (about 2%) and practically does not influence the oscillation amplitude.

#### Effect of the solute/solution properties and comparison with experimental data

The bulk diffusion coefficient and the solution viscosity are included in the Schmidt and Marangoni numbers. An increase of the diffusion coefficient leads to a decrease of both numbers and therefore to an increase of the dimensionless induction and oscillation period. At the same time, the diffusion coefficient is part of the scaling factor for the time. The last effect is much stronger and the dimensional values

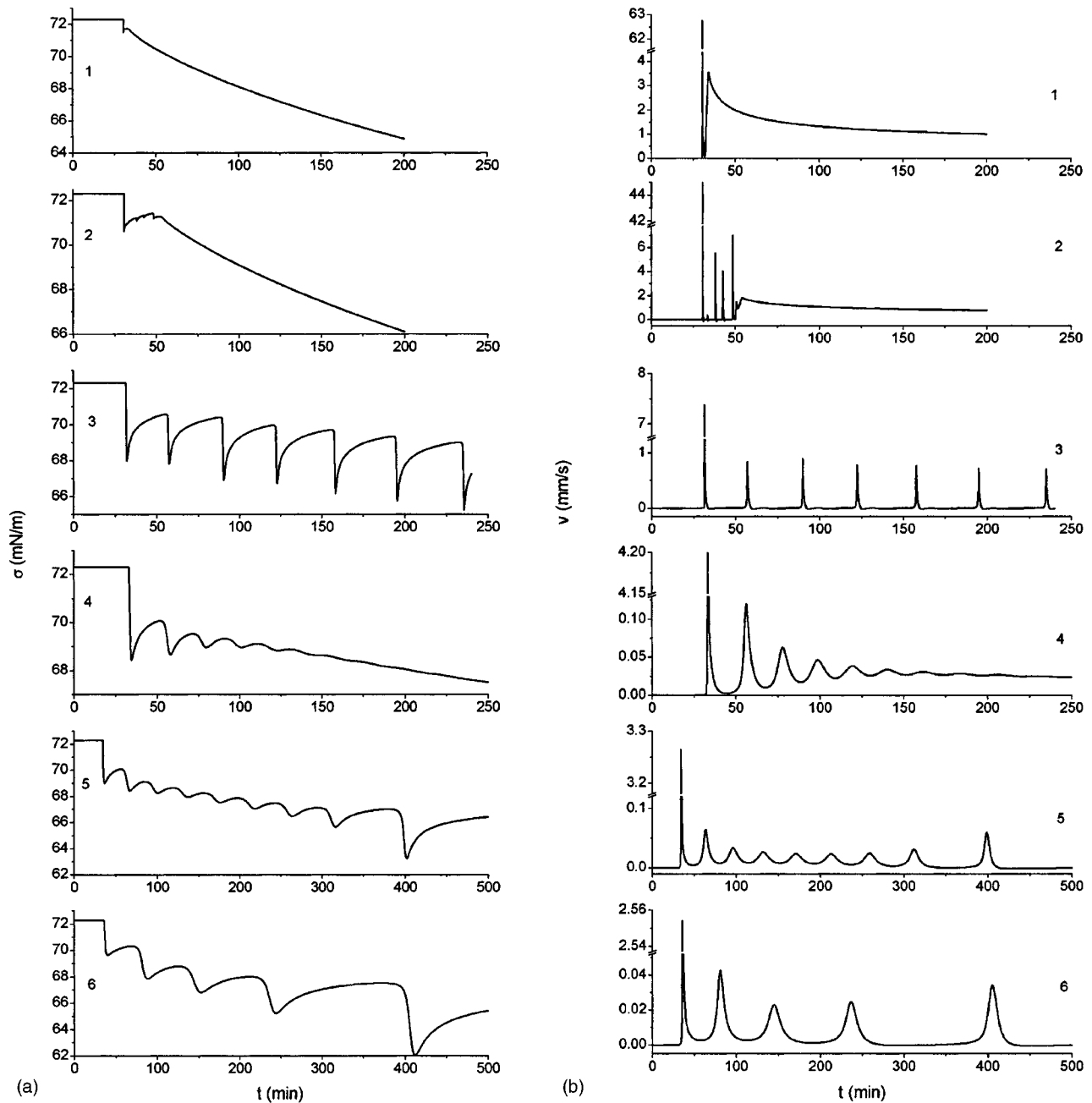


FIG. 6. Surface tension (a) and surface velocity (b) vs time for  $Ma=5.4 \times 10^9$ ,  $Sc=1500$ : 1,  $N_E=94\,000$ ; 2,  $N_E=47\,000$ ; 3,  $N_E=940$ ; 4,  $N_E=190$ ; 5,  $N_E=94$ ; 6,  $N_E=47$ .

of the period decrease with an increase of the diffusion coefficient. The system passes to the nonoscillating regime at  $D$  larger than some critical value depending on the other system characteristics. The results are clear from a physical point of view: the mass transfer during the slow stage becomes faster when the diffusion coefficient increases, resulting in a decrease of the induction period and the oscillation period. At large enough diffusion coefficient, the reverse concentration gradient occurring near the wall due to convection is destroyed rather quickly by diffusion, which prevents the development of the reverse convective roll and leads to nonoscillating system evolution. The oscillation amplitude decreases with an increase of the diffusion coefficient

rather slowly in accordance with the opposite effects of the Marangoni and the Schmidt numbers.

An increase of the solution viscosity leads to an increase of the Schmidt number and to a decrease of the Marangoni number. In this case, both numbers influence the amplitude change in the same direction, and the amplitude increases considerably with the viscosity increase. The induction period increases as well in accordance with the stronger influence of the Marangoni number on this characteristic. Most complicated is the viscosity effect on the oscillation period. A decrease of the Marangoni number causes an increase of the oscillation period. An increase of the Schmidt number from 1500 to 15 000 leads to the same result. Thus, at large

TABLE V. Effect of the solute/solution properties on the oscillation characteristics.

Property (increase of the values)	Induction period	Oscillation period	Oscillation amplitude	Nonoscillating regime
Bulk diffusion coefficient $\uparrow$	$\downarrow$	$\downarrow$	$\downarrow$	$D > D_{\text{crit}}$
Solution viscosity $\uparrow$	$\uparrow$	$\uparrow$ at large $\mu$ $\downarrow$ at small $\mu$	$\uparrow$	$\nu < \nu_{\text{crit}}$
Solution density $\uparrow$	$\uparrow$	$\uparrow$ at large $\rho$ $\downarrow$ at small $\rho$	$\downarrow$	$\rho > \rho_{\text{crit}}$
Surfactant activity ( $\alpha = K_L \Gamma_m$ ) $\uparrow$	$\downarrow$	$\uparrow$	$\uparrow$	$\alpha < \alpha_{\text{crit1}}$ $\alpha_{\text{crit2}} < \alpha < \alpha_{\text{crit3}}$ ( $\alpha_{\text{crit1}} < \alpha_{\text{crit2}}$ )
Surfactant solubility $\uparrow$	$\downarrow$	$\downarrow$	$\uparrow$	

enough solution viscosities (larger than water viscosity in the considered parameter range), the oscillation period increases with viscosity increase. On the contrary, at small solution viscosities, the viscosity increase leads to a weak decrease of the oscillation period due to the stronger effect of the Schmidt number. When the solution viscosity is smaller than a certain critical value, the system passes to the nonoscillating regime due to a decrease of the feedback between concentration gradient and velocity.

An increase of the solution density leads to a decrease of the Schmidt number and therefore to a decrease of the oscillation amplitude and to a weak increase of the induction period. The oscillation period increases with density increase at its large values (compared to water density) and decreases at small values. The system passes to a nonoscillatory state at large enough solution densities.

The effect of the Langmuir isotherm parameters  $\Gamma_m$  and  $K_L$  on the auto-oscillations characteristics is very similar, which is why we will consider here only the effect of the surfactant activity  $\alpha = K_L \Gamma_m$ . An increase of the surfactant activity leads to an increase of the Marangoni number and to a decrease of the exchange number. As a result, the induction period decreases with activity increase according to the stronger influence of the Marangoni number on this characteristic, but the oscillation period increases due to the stronger influence of the exchange number. The dimensional oscillation amplitude increases due to the stronger influence of the exchange number and mainly due to scaling of adsorption by  $c_0 K_L \Gamma_m$ . The nonoscillatory regime can appear at small activities as well as in a certain range of the middle parameter values.

The surfactant solubility is included only in the Marangoni number. Therefore, the induction period and oscillation period decrease with an increase of the solubility, and the oscillation amplitude increases considerably, especially

due to scaling of adsorption by  $c_0 K_L \Gamma_m$ . The influence of the system properties on the oscillation characteristics is summarized in Table V.

The surfactant solubility and the parameter of Langmuir isotherm  $K_L$  are also included in the multiplier  $1/(1 - K_L c_0 \Gamma) = (1 + K_L c_0 c)|_{z=0}$ , which, together with the Marangoni number, appears in the equation of tangential stress balance (5). Obviously, the effect of this multiplier is negligible during the induction period, when the surfactant concentration at the interface is very small, which is confirmed by results of the numerical simulation. At the same time, this multiplier influences the oscillation period strongly enough. An increase of the value  $K_L c_0$  leads to a decrease of the oscillation period. The effect of the surfactant solubility is especially important, as the influence of the Marangoni number on the oscillation period is rather weak. For example, as is seen from Table II, an increase on the Marangoni number from  $5.4 \times 10^9$  to  $5.4 \times 10^{10}$  leads to a decrease of the oscillation period from 36 min to 35 min, whereas the corresponding increase of the surfactant solubility (from  $c_0 = 3.4 \text{ mol/m}^3$  to  $c_0 = 34 \text{ mol/m}^3$ ) causes a decrease of the oscillation period to 19 min. The influence of the multiplier  $1/(1 - K_L c_0 \Gamma)$  due to a change of  $K_L$  is less essential in comparison to the effect of the exchange number.

The effect of surfactant properties on the auto-oscillations characteristics was studied experimentally for the series of the middle chain aliphatic alcohols [18]. It was established that the oscillation period (as well as the induction period) decreases rather strongly with a decrease of the alcohol chain length. That is, it changes from about 15 min for nonanol to less than 1 min for pentanol. The oscillations amplitude also decreases, but much more slowly.

Dependence of the surface tension versus time was calculated by using the mathematical model proposed in [21] for three surfactants, taking the properties of octanol, heptanol, and hexanol given in [18] (Table VI).

TABLE VI. Properties of the middle chain aliphatic alcohols [18].

Substance	$\rho$ (g/cm <sup>3</sup> )	$D$ (10 <sup>-6</sup> cm <sup>2</sup> /s)	$c_0$ (10 <sup>-6</sup> mol/cm <sup>3</sup> )	$K_L$ (10 <sup>6</sup> cm <sup>3</sup> /mol)	$\Gamma_m$ (10 <sup>-10</sup> mol/cm <sup>2</sup> )
octanol	0.827	6.67	3.4	3.23	6.6
heptanol	0.822	7.18	14	0.62	7.7
hexanol	0.819	7.81	58	0.23	6.2

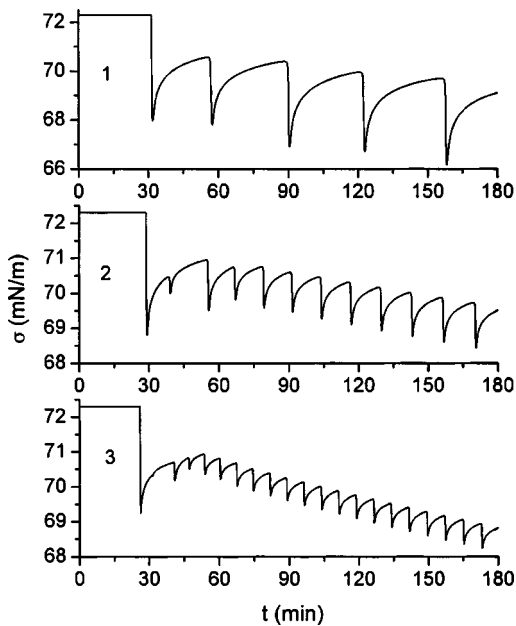


FIG. 7. Surface tension vs time (numerical results): 1, octanol; 2, heptanol; 3, hexanol.

A simple analysis of the data of Table VI shows that the values of the Schmidt and Marangoni numbers as well as the multiplier  $1/(1 - K_L c_0 \Gamma)$  differ insignificantly for the three chosen substances. The difference in the diffusion coefficients should lead to small increase of the oscillation period with an increase of the chain length according to the time scaling. The difference in the oscillations characteristics is determined mainly by the change of the exchange number. By invariable system geometry, the exchange number decreases with an increase of the alcohol chain length. Therefore, the calculated values of the oscillation period and amplitude as well as the value of the induction period (to a lesser extent) increase with an increase of the alcohol chain length (Fig. 7). The calculated value of the critical capillary immersion depth, which, when exceeded, causes the system to pass from a nonoscillatory to an oscillatory regime, decreases with an increase of the alcohol chain length (cell radius is kept constant), which corresponds to experiments. The obtained numerical results are in good qualitative agreement with the experimental data. However, to reach a quantitative agreement, a more complicated mathematical model is needed, which takes into account the buoyancy effect as well as such other effects as surfactant evaporation and interface deformation.

## CONCLUSIONS

Numerical simulation of the processes occurring in the system where a surfactant droplet is dissolved under the water-air interface is fulfilled on the basis of the mathematical model, taking into account the convection driven by the Marangoni effect and convective diffusion together with adsorption/desorption processes at the air-water interface. It is shown that the system behavior is determined by three of

the dimensionless parameters: the Marangoni number, the Schmidt number, and the exchange number. The effect of the ratio of the surface and the bulk diffusion coefficients, which also appears by the dimensionalization of the governing equations, is practically negligible.

The Schmidt number influence is rather small for the induction period and the oscillation period. The oscillation amplitude increases with an increase of the Schmidt number. When the parameter value becomes less than a certain critical value, the system passes to the nonoscillatory state.

The Marangoni number, which appears in the dimensionless form of the surface stress balance equation, is a global number and characterizes the system as a whole. The onset of instability in the system is determined by the local Marangoni number, which is a product of the global number and the dimensionless normal concentration gradient near the surface. The local Marangoni number in the considered system depends on coordinates and changes with time. The larger the global Marangoni number is, the smaller is the normal concentration gradient needed to reach the critical value of the local Marangoni number. That is why the induction period and the oscillation period decrease with an increase of the global Marangoni number. The oscillation amplitude decreases rather weakly with an increase of the Marangoni number. Only oscillatory regimes are obtained for the studied range of the Marangoni numbers.

The exchange number determines the solute flux from the bulk to the interface or back. It practically does not influence the induction period, but the oscillation period and amplitude decrease strongly by an increase of the exchange number. The way in which the system goes to the final equilibrium concentration distribution depends essentially on the exchange number. When it exceeds a certain critical value, the system passes to the nonoscillatory regime. There is also a region of the middle values of the exchange numbers where oscillations are damped very quickly.

The critical value of the local Marangoni number depends on the exchange number, pointing out that the value of the flux to the interface rather than the concentration gradient is responsible for the instability onset.

Analysis of the numerical results permits us to establish a criterion for the instability onset in the considered system, where the convective motion develops initially due to the tangential concentration gradient. In the considered system, the growth rate of the stable convection decreases with time, and the time moment corresponding to the minimum of the velocity growth rate can be accepted as an estimated (from above) value for the instability onset.

The effect of substance properties on the appearance and characteristics of the surface tension auto-oscillation is also studied. The induction period decreases with an increase of the bulk diffusion coefficient, surfactant activity, and solubility, but increases with an increase of the solution viscosity and density. The oscillation period decreases with an increase of the bulk diffusion coefficient and surfactant solubility, but increases with an increase of the solution viscosity and density (with the only exception being small viscosities and densities) and surfactant activity. The oscillation ampli-

tude increases with an increase of the solution viscosity, surfactant activity, and solubility, but decreases with an increase of the bulk diffusion coefficient and solution density. There exist critical values of the bulk diffusion coefficient, surfactant activity, solution viscosity, and density that divide the oscillatory and nonoscillatory path in the system evolution. The critical values depend on other substance properties.

The results of the numerical simulations are in good qualitative agreement with the experimental data for aliphatic alcohols.

#### ACKNOWLEDGMENT

N.M.K. gratefully thanks the Max Planck Institute of Colloids and Interfaces for financial support of this work.

- 
- [1] E.L. Koschmieder, *Benard Cells and Taylor Vortices* (Cambridge University Press, Cambridge, 1993).
- [2] *Convective Transport and Instability Phenomena*, edited by J. Zieper and H. Oertel (Braun, Karlsruhe, 1982).
- [3] J.R.A. Pearson, *J. Fluid Mech.* **4**, 489 (1958).
- [4] C.V. Sternling and L.E. Scriven, *AIChE J.* **5**, 514 (1959).
- [5] D.A. Nield, *J. Fluid Mech.* **19**, 341 (1964).
- [6] J. Bragard, S.G. Slavtchev, and G. Lebon, *J. Colloid Interface Sci.* **168**, 402 (1994).
- [7] A. Engel and J.B. Swift, *Phys. Rev. E* **62**, 6540 (2000).
- [8] P.S. Dauby, Th. Desaive, J. Bragard, and P. Cerisier, *Phys. Rev. E* **64**, 066301 (2001).
- [9] S.H. Strogatz, *Nonlinear Dynamics and Chaos* (Perseus Books, Cambridge, MA, 1994).
- [10] M. Dupeyrat and E. Nakache, *Bioelectrochem. Bioenerg.* **5**, 134 (1978).
- [11] E. Nakashe, M. Dupeyrat, and M. Vignes-Adler, *J. Colloid Interface Sci.* **94**, 187 (1983).
- [12] S. Kai, T. Mori, and M. Miki, in *Pattern Formation in Complex Dissipative Systems*, edited by S. Kai (World Scientific, Singapore, 1992); S. Kai, S.C. Muller, T. Mori, and M. Miki, *Physica D* **50**, 412 (1991).
- [13] N. Magome and K. Yoshikawa, *J. Phys. Chem.* **100**, 19102 (1996).
- [14] K. Arai and F. Kusu, in *Liquid Interfaces in Chemical, Biological and Pharmaceutical Applications (Surf. Sci. Series/95)*, edited by A.G. Volkov (Dekker, New York, 2001).
- [15] K. Maeda, S. Nagami, Y. Yoshida, H. Ohde, and S. Kihara, *J. Electroanal. Chem.* **496**, 124 (2001).
- [16] A. Shioi, H. Kumagai, Y. Sugiura, and Y. Kitayama, *Langmuir* **18**, 5516 (2002).
- [17] V.I. Kovalchuk, H. Kamusewitz, D. Vollhardt, and N.M. Kovalchuk, *Phys. Rev. E* **60**, 2029 (1999).
- [18] N.M. Kovalchuk and D. Vollhardt, *J. Phys. Chem. B* **104**, 7987 (2000).
- [19] N.M. Kovalchuk and D. Vollhardt, *Mater. Sci. Eng. C* **22**, 147 (2002).
- [20] T. Takahashi, H. Yui, and T. Sawada, *J. Phys. Chem. B* **106**, 2314 (2002).
- [21] N.M. Kovalchuk and D. Vollhardt, *Phys. Rev. E* **66**, 026302 (2002).
- [22] N.M. Kovalchuk and D. Vollhardt, *J. Phys. Chem. B* **107**, 8439 (2003).